

Excited-State Energy Transfer Processes in Phenylene- and Biphenylene-Linked and Directly-Linked Zinc(II) and Free-Base Hybrid Diporphyrins

Hyun Sun Cho,[†] Dae Hong Jeong, Min-Chul Yoon, Yong Hee Kim, Yong-Rok Kim,[‡] and Dongho Kim*

Center for Ultrafast Optical Characteristics Control and Department of Chemistry, Yonsei University, Seoul 120-749, Korea

Sae Chae Jeoung

Korea Research Institute of Standards and Science, Taejeon 305-600, Korea

Seong Keun Kim

School of Chemistry, Seoul National University, Seoul 151-742, Korea

Naoki Aratani, Hideyuki Shinmori, and Atsuhiko Osuka*

Department of Chemistry, Graduate School of Science, Kyoto University, Kyoto 606-8502, Japan

Received: January 31, 2001

The photoinduced energy transfer processes in 1,4-phenylene-, 1,3-phenylene, 1,2-phenylene, and 4,4'-biphenylene-linked and directly-linked Zn(II)-free base porphyrin heterodimers in THF were investigated by femtosecond transient absorption spectroscopy. The energy transfer rates were compared between TPP-type and OEP-type heterodimers respectively as A_{2u}-HOMO and A_{1u}-HOMO subunits, for evaluating the relative contribution of the through-bond and through-space interactions. The rate difference becomes smaller with a decrease of spacer, more than 10 for 1,4-bis(phenylethynyl)phenylene and 1,4-diphenylethynylene, 4 for 4,4'-biphenylene-linked heterodimer, and 3 for 1,3- and 1,4-phenylene-linked spacers. In the meso–meso directly-linked case, the energy transfer rates are the same ((0.55 ps)⁻¹) for 5,5,15,15-tetrakis(3,5-bis(octyloxy)phenyl)-substituted and 5,5,15,15-tetrakis(pentafluorophenyl)-substituted heterodimers, featuring only a minor influence of the frontier orbital characteristics on the energy transfer rate. The energy transfer rates are identical (0.55 ps)⁻¹ for the directly-linked meso–meso heterodimers substituted with 3,5-bis(octyloxy)phenyl and pentafluorophenyl groups regardless of the difference in the HOMO orbital symmetry characteristics, suggesting the predominant Coulombic interaction for the energy transfer in these close proximity porphyrin dimers. In the case of 1,2-phenylene-linked heterodimers, the choice of the peripheral substituents can lead to a state-to-state rapid energy transfer with a rate of (0.55 ps)⁻¹ for the TPP-type model or a delocalized excimer-like diporphyrin excited state for the OEP-type model. Collectively, these results indicate that even for the covalently-linked models the relative contribution of the through-space Coulombic interaction becomes increasingly important upon the decrease of the center-to-center separation. Especially, the fast and efficient energy transfer occurring in the directly-linked heterodimer illustrates that this porphyrin unit can be utilized as a good candidate for energy transfer functional arrays in molecular photonic devices.

I. Introduction

A variety of porphyrin arrays have been synthesized as artificial photosynthetic models capable of forming long-lived charge-separated states upon photoexcitation and as artificial antenna of harvesting and transmitting light energy along the designed direction, in which porphyrin units are joined together by using various types of linkers in linear or extended architectures via meso position attachment.^{1–10} These porphyrin arrays may have potential uses for molecular photonic devices such as molecular wires, switches, logic gates, and so on.^{2,3} Since the efficiency of light-harvesting and signal transmission

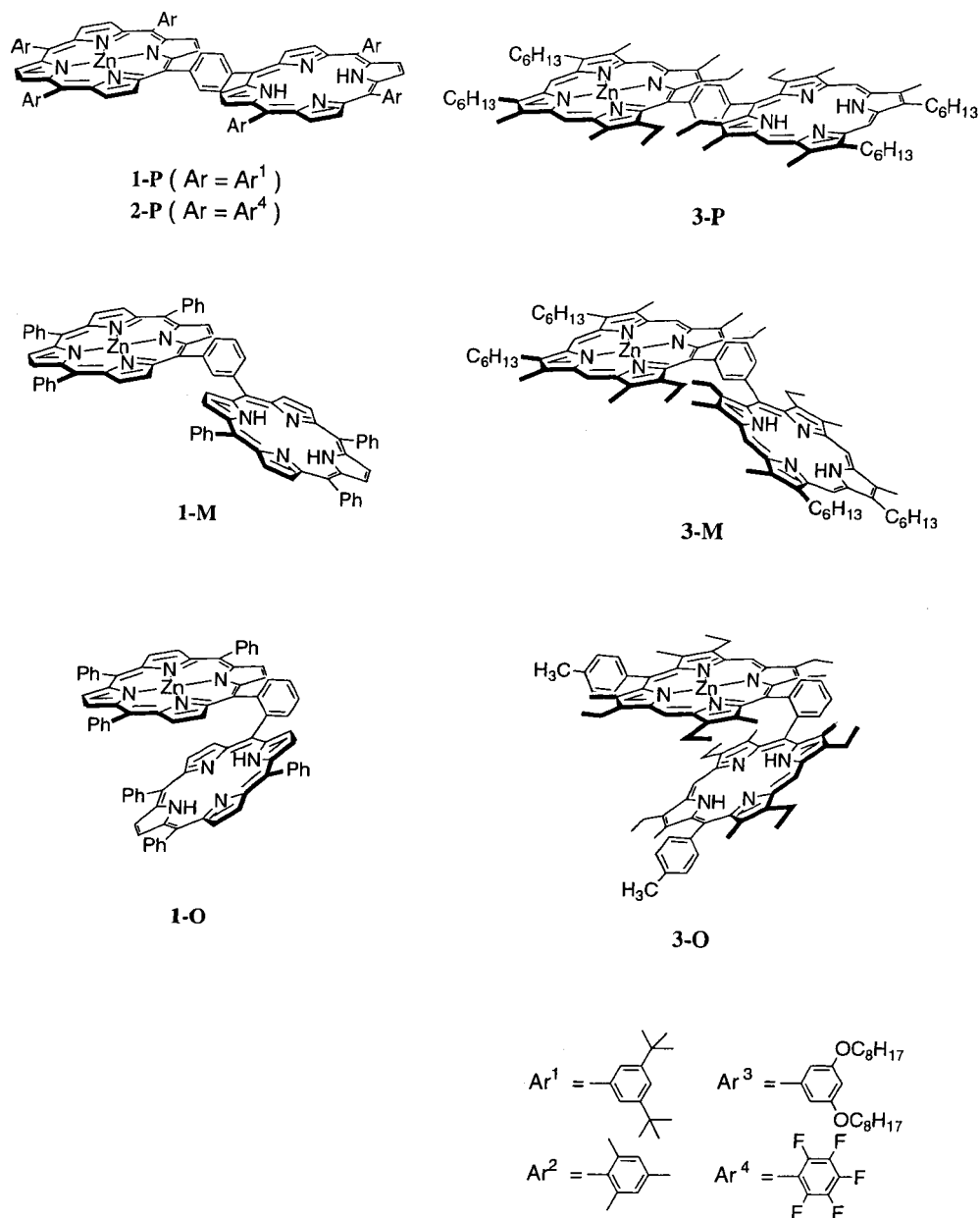
in molecular photonic devices relies heavily on the light energy transfer process, understanding of the key elements in *inter*-porphyrin energy transfer in porphyrin arrays is indispensable for the realization of artificial antenna and molecular photonic devices. Generally, the two types of the electronic interactions are identified for the energy transfer processes; one is the Coulombic interaction affected by the through-space coupling of transition dipole moments via oscillating electromagnetic field¹¹ and the other is the electron exchange interaction that is provided by direct or indirect overlap of wave functions.¹² These two interactions are often considered respectively to be a dominant factor for the Förster and Dexter mechanism. On the basis of the different electronic interaction origins, it is qualitatively considered for energy transfer in noncovalent donor–acceptor pairs that the Förster mechanism can be

* To whom correspondence should be addressed.

[†] Also with Department of Chemistry, Seoul National University, Seoul 151-742.

[‡] Department of Chemistry, Yonsei University, Seoul 120–749.

SCHEME 1

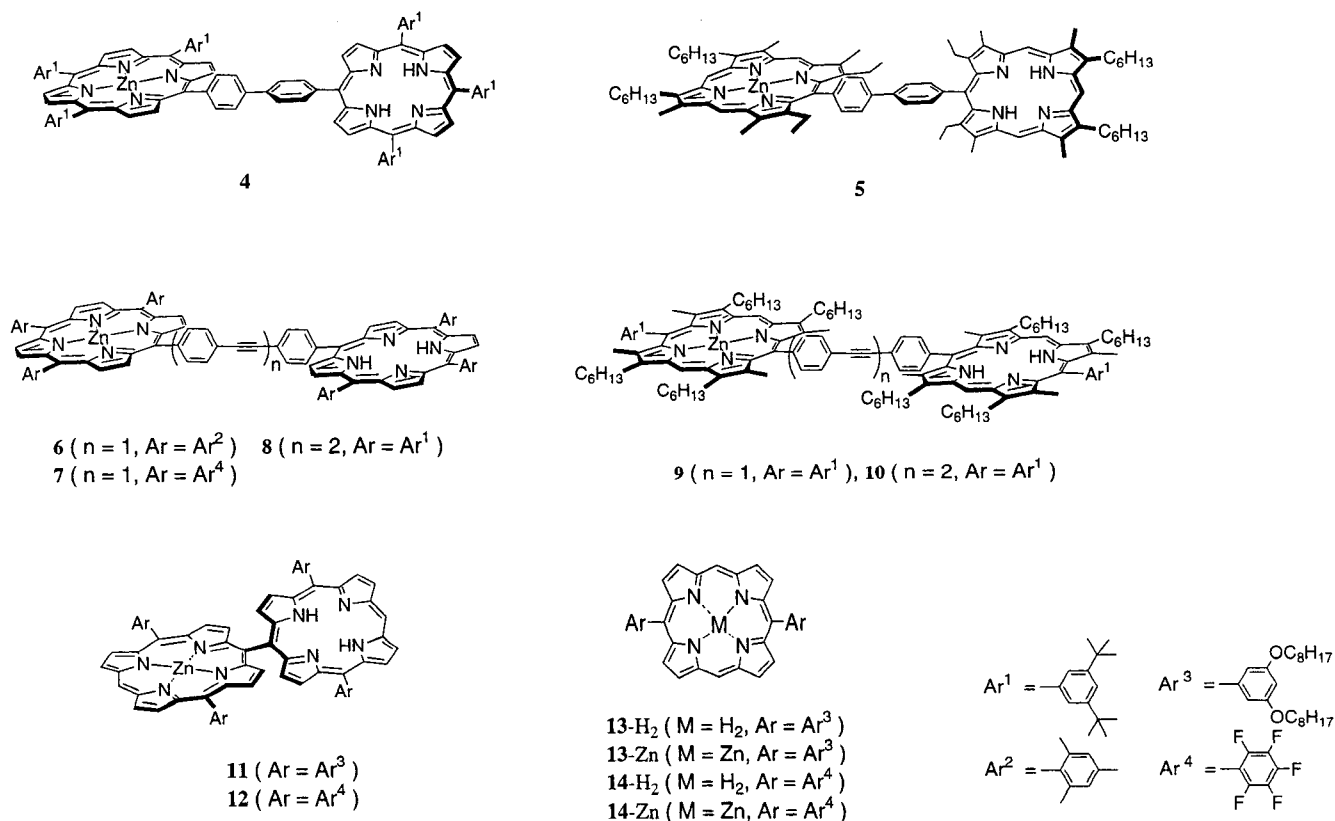


operative at a long distance, while the Dexter mechanism can be effective only at a short distance.^{11,12} In natural systems where chromophores are usually not covalently linked but held at an appropriate distance and orientation by the protein matrix, most of the energy transfer processes can be considered to be driven by Coulombic interactions, covering a wide range of phenomena¹³ from relatively slow processes as such in the Förster mechanism to rather rapid energy transfers between neighboring chromophores in C-phycoyanintrimers,¹⁴ from the accessory bacteriochlorophyll to the special pair in bacterial photosynthetic reaction center,¹⁵ and from B800 to B850 energy transfer in LH2.¹⁶ In model studies, however, the energy transfer reactions have been extensively studied for cases with center-to-center distance, $R > 20 \text{ \AA}$ and only scattered systematic studies have been made for the distance dependence for $R < 20 \text{ \AA}$.¹ Therefore, systematic studies on a state-to-state energy transfer with close proximity are quite important for understanding of the key mechanism of the natural light-harvesting processes. A related and interesting question may be the closest limit of a state-to-state energy transfer process of chlorophyll and por-

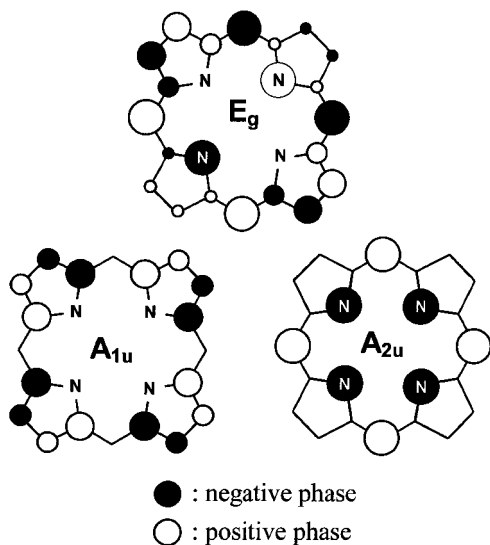
phyrin pigments, since too close proximity may inevitably lead to a strongly interacting dimer with significantly altered spectral characteristics better characterized by the excitonic coupling.

On the other hand, the impact of a covalent linkage in synthetic models is quite significant, in that the covalent bonds between a donor and an acceptor provide a way for efficient transmission of the electron exchange interactions over long distance (Schemes 1 and 2). This feature is more evident for donor-acceptor models bridged by π -conjugated linkers.¹⁷⁻²⁰ The distance dependency of the energy transfer processes over the π -conjugated bridges has been actually demonstrated to be quite small; the attenuation factors were reported to be 0.08 and 0.1 \AA^{-1} for diphenylpolyene and diphenylpolyyne spacers, respectively.¹⁷ These results revealed the efficient transmission capability of electron exchange interaction through these π -conjugated bridges, which is in line with the dominant Dexter mechanism. The dominant contribution of the Dexter mechanism was also reported on the basis of remarkable differences between the energy transfer rates of 4,4'-diphenylethynyl-bridged Zn(II)-free base hybrid diporphyrins **6** and **9**¹⁸ and between those

SCHEME 2



SCHEME 3



of bis(phenylethynyl)phenylene-bridged hybrid diporphyrins **8** and **10**¹⁹ (Scheme 2). The energy transfer rates were reported to be $(24 \text{ ps})^{-1}$ and $(417 \text{ ps})^{-1}$ for **6** and **9**, and $(156 \text{ ps})^{-1}$ and $(1750 \text{ ps})^{-1}$ for **8** and **10**, respectively.^{17–19} Lindsey et al.¹⁸ have ascribed these differences to the reversal of the HOMO orbital of the porphyrin components, which is accompanied by the change of porphyrin peripheral substituents. TPP-type Zn(II) porphyrins have an A_{2u} HOMO orbital with substantial electron density at the meso positions where the diarylethynyl spacer is connected, while a 5,15-diaryl- β -octaalkyl Zn(II) porphyrin has A_{1u} HOMO orbitals with a node at the meso positions (Scheme 3). The observed slow energy transfer rate $(240 \text{ ps})^{-1}$ of the corresponding hexakis(pentafluorophenyl)-substituted Zn(II)-free base hybrid diporphyrin **7** has been also ascribed to its A_{1u}

HOMO orbital, which is unfavorable for through-bond electronic communication.¹⁸

Placement of a donor and an acceptor in a closer proximity is another way to enhance the rate of energy transfer, as seen in the natural systems. This enhancement is caused mostly through the increase of the through-space Coulombic interactions, which can become increasingly important with a decrease in a distance as suggested in B800–B850 in LH2¹⁶ and carotenoid-to-bacteriochlorophyll.^{21,22} A geometrically well-defined covalently-linked synthetic model would be very useful for study on the energy transfer occurring in such a close proximity system, but the difficulty in evaluating the relative contribution of the through-space and through-bond interactions in the overall electronic interactions has left the systematic study on the Coulombic interactions in the energy transfer almost untouched. Such a study would be important from different viewpoints of increasing the energy transfer rate that can rival the natural ultrafast energy transfer and of exploring the closest limit of photosynthetic pigments for a state-to-state energy transfer.

With these backgrounds in mind, the main aims of the present study are to explore an efficient state-to-state energy transfer and reveal the dominant factor that is responsible for such a rapid energy transfer. More specifically, we want to evaluate the relative importance of Coulombic interaction in the extremely fast energy transfer in a close proximity with respect to the through-bond electronic interactions. In the present study, we have prepared two sets of Zn(II)-free base hybrid diporphyrins linked by 1,2-, 1,3-, and 1,4-phenylene spacers (**1-P**, **1-M**, **1-O**, **3-P**, **3-M**, and **3-O**),^{23–28} as shown in Scheme 1 and two 4,4'-biphenylene-linked hybrid diporphyrins (**4** and **5**) and directly meso–meso-linked hybrid diporphyrins **11** and **12** as a spacerless extreme case (Scheme 2).²⁹ The model **12** was employed in order to investigate the electronic effects on the

energy transfer rate, since the Zn(II) porphyrin subunit in **12** is expected to have an A_{1u} HOMO orbital owing to strongly electron withdrawing pentafluorophenyl substituents as such in **7**.

II. Experimental Section

Synthesis. Detailed synthetic procedures are given in the Supporting Information.

Absorption and Fluorescence Spectroscopic Measurements. UV-visible spectra were recorded with a Shimadzu UV-2400 spectrometer and steady-state fluorescence spectra were taken on a Shimadzu RF-5300 spectrofluorometer in THF.

Transient Absorption Experimental Setup. The dual-beam femtosecond time-resolved transient absorption spectrometer consisted of a self-mode-locked femtosecond Ti:sapphire laser (Clark MXR, NJA-5), a Ti:sapphire regenerative amplifier (Clark MXR, CPA-1000) pumped by a Q-switched Nd:YAG laser (ORC-1000), a pulse stretcher/compressor, OPG-OPA system, and an optical detection system. A femtosecond Ti:sapphire oscillator pumped by a CW Nd:YVO₄ laser (Spectra Physics, Millennia) produces a train of 60 fs mode-locked pulses with an averaged power of 250 mW at 800 nm. The seed pulses from the oscillator were stretched (~250 ps) and sent to a Ti:sapphire regenerative amplifier pumped by a Q-switched Nd:YAG laser operating at 1 kHz. The femtosecond seed pulses and Nd:YAG laser pulses were synchronized by adjusting an electronic delay between Ti:sapphire oscillator and Nd:YAG laser. Then the amplified pulse train inside the Ti:sapphire regenerative amplifier cavity was cavity-dumped by using Q-switching technique, and about 30 000-fold amplification at 1 kHz was obtained. After recompression, the amplified pulses were color-tuned by optical parametric generation and optical parametric amplification (OPG-OPA) technique. The resulting laser pulses had a pulse width of ~150 fs and an average power of 5–30 mW at 1 kHz repetition rate in the range 550–700 nm. The pump beam was focused to a 1 mm diameter spot, and the laser fluence was adjusted less than ~1.0 mJ/cm² by using a variable neutral-density filter. The fundamental beam remaining in the OPG-OPA system was focused onto a flowing water cell to generate white continuum, which was again split into two parts. The one part of the white light continuum was overlapped with the pump beam at the sample to probe the transient, while the other part of the beam was passed through the sample without overlapping the pump beam. The time delay between pump and probe beams was controlled by making the pump beam travel along a variable optical delay. The white continuum beams after the sample were sent to a 15 cm focal length spectrograph (Acton Research) through each optical fiber and then detected by the dual 512 channel photodiode arrays (Princeton Instruments). The intensity of the white light of each 512 channel photodiode array was processed to calculate the absorption difference spectrum at the desired time delay between pump and probe pulses.

III. Results

Transient Absorption Spectra of Phenylene-Bridged Diporphyrins. The absorption spectra of various Zn(II)-free base hybrid diporphyrins in the Q-band region are essentially given by the sum of the spectrum of each constituent except the case of **3-O** (Figures 1–6). The Q-bands of **3-O** are extremely broad and featureless, indicating the strongest electronic interactions between the adjacent porphyrins in the series. On the other hand, the Soret bands of these diporphyrins are characterized by the exciton coupling which causes a band splitting for **1-P** and **1-M**

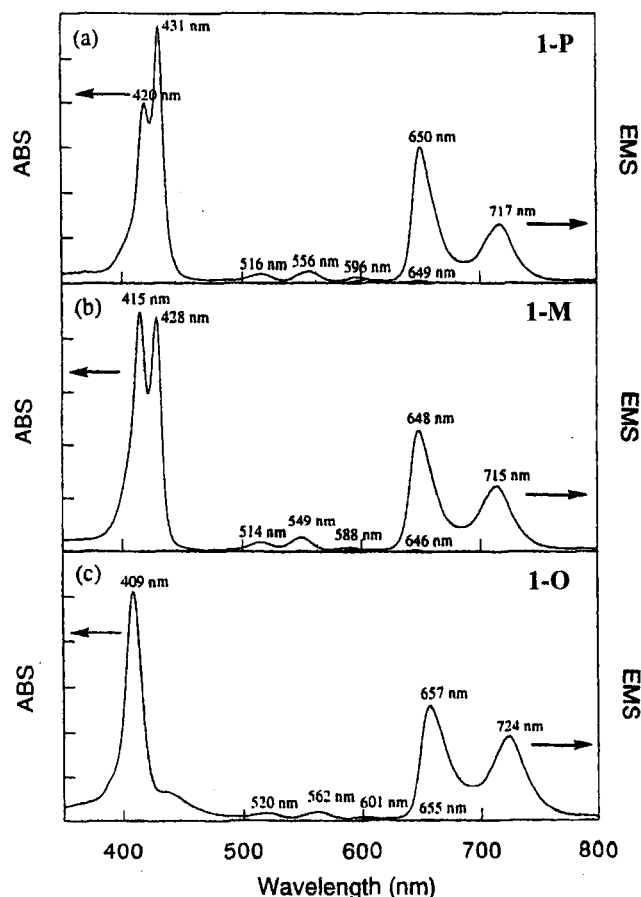


Figure 1. Absorption and emission spectra of various TPP-typed Zn(II)-free base diporphyrin dimers with phenylene spacer, (a) **1-P**, (b) **1-M**, and (c) **1-O** in THF. Emission spectra are obtained by exciting the Zn(II) porphyrin at 550 nm.

and a band broadening for **3-P** and **3-M** and a blue-shift for **1-O** and **3-O**, respectively.^{8d} The strength of exciton coupling is mainly determined by the center-to-center distance between the porphyrin monomers.³⁰ These characteristics indicate relatively weak electronic interactions between monomeric constituents for **1-P**, **1-M**, **3-P**, and **3-M**, which enables a selective photoexcitation of the high-energy Zn(II) porphyrin unit to track down the energy flow from the photoexcited Zn(II) porphyrin to the free-base porphyrin by measuring the time evolution of transient absorption spectral changes. Such a selective excitation at the Zn(II) porphyrin moiety is also possible for **1-O** but rather difficult for **3-O** due to the spectral broadening. In the steady-state fluorescence measurements of various Zn(II)-free base hybrid diporphyrins, the fluorescence emission comes predominantly from free base porphyrin, indicating that the energy transfer occurs efficiently from photoexcited high-energy Zn(II) porphyrin to ground-state low-energy free base porphyrin (Figures 1–7).

The energy transfer rates and efficiencies in various Zn(II)-free base diporphyrins in THF were investigated quantitatively by employing femtosecond pump/probe transient absorption difference measurements. The first example is the energy transfer in 1,4-phenylene-bridged **1-P** (Figure 8a).^{25b} The overall transient absorption spectra at 1.4 ps time delay between pump and probe pulses after selective photopumping of Zn(II) porphyrin unit at ~556 nm exhibits the bleaching of the moderately strong Q(1,0) band near 556 nm, flanked by bleachings of the weak Q(2,0) and Q(0,0) bands at ~516 and ~596 nm, respectively. Nearly half of the bleaching signal near

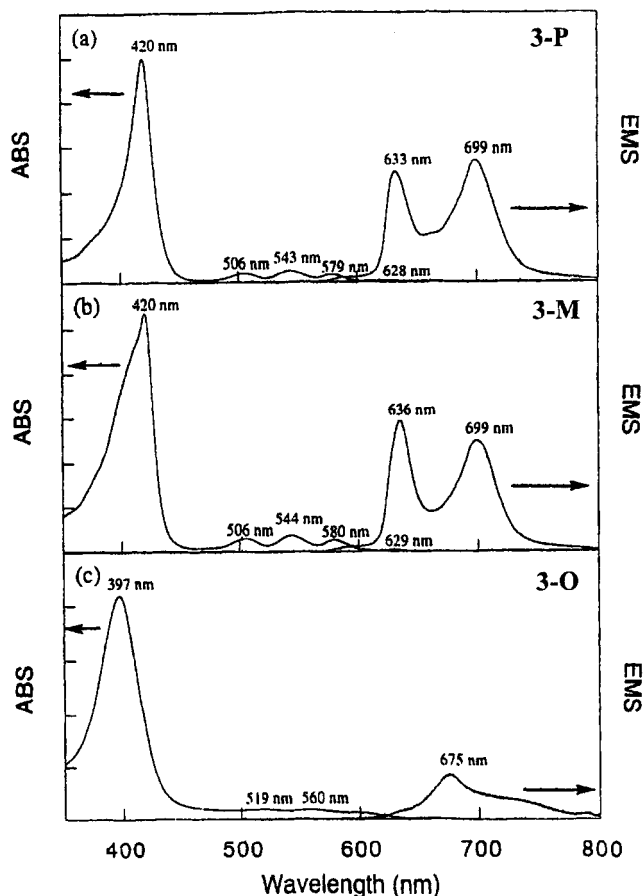


Figure 2. Absorption and emission spectra of various OEP-typed Zn(II)-free base diporphyrin dimers with phenylene spacer, (a) **3-P**, (b) **3-M**, and (c) **3-O** in THF. Emission spectra are obtained by exciting the Zn(II) porphyrin at 580 nm.

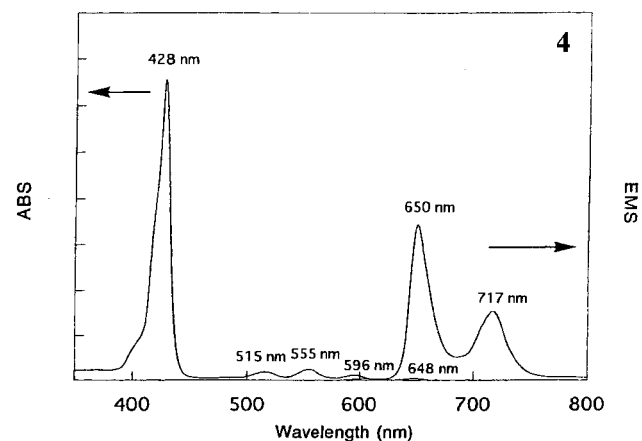


Figure 3. Absorption and emission spectra of TPP-typed Zn(II)-free base diporphyrin dimer with diphenylene spacer, **4** in THF. The emission spectrum is obtained by exciting the Zn(II) porphyrin at 550 nm.

596 nm arises from photoexcited Zn(II) porphyrin Q(0,0) stimulated emission induced by the white light continuum pulses. This spectral feature suggests that the transient absorption spectrum at 1.4 ps time delay is primarily contributed by the photoexcited Zn(II) porphyrin unit along with a nonnegligible contribution of a slight amount of photoexcited free base porphyrin. This feature can be seen by a small bleaching signal at ~ 516 nm at early delay time, which is due to the $Q_y(1,0)$ ground-state absorption band of free base porphyrin. An increase in the delay time results in an increase in the contribution of

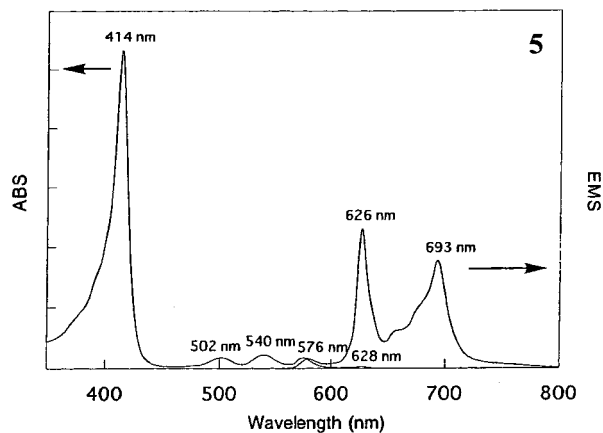


Figure 4. Absorption and emission spectra of OEP-typed Zn(II)-free base diporphyrin dimer with diphenylene spacer, **5** in THF. The emission spectrum is obtained by exciting the Zn(II) porphyrin at 580 nm.

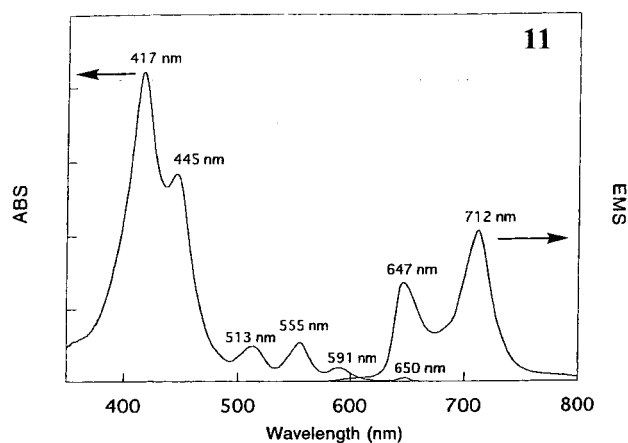


Figure 5. Absorption and emission spectra of directly-linked Zn(II)-free base diporphyrin dimer **11** in THF. The emission spectrum is obtained by exciting the Zn(II) porphyrin at 550 nm.

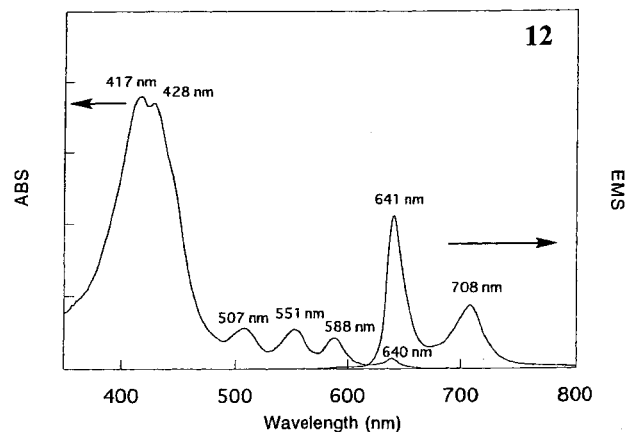


Figure 6. Absorption and emission spectra of directly-linked pentafluorophenyl substituted Zn(II)-free base diporphyrin dimer **12** in THF. The emission spectrum is obtained by exciting the Zn(II) porphyrin at 550 nm.

free base porphyrin transient to the overall transient absorption spectrum, as indicated by the growth of the 516 nm bleaching of free base porphyrin. At its expense, the bleaching signal at 556 nm by Zn(II) porphyrin diminishes upon increasing the delay time. At the longer time delay of ~ 9.0 ps, the overall spectral feature is dominated by free base porphyrin, as characterized by the full growth of free base bleaching band at

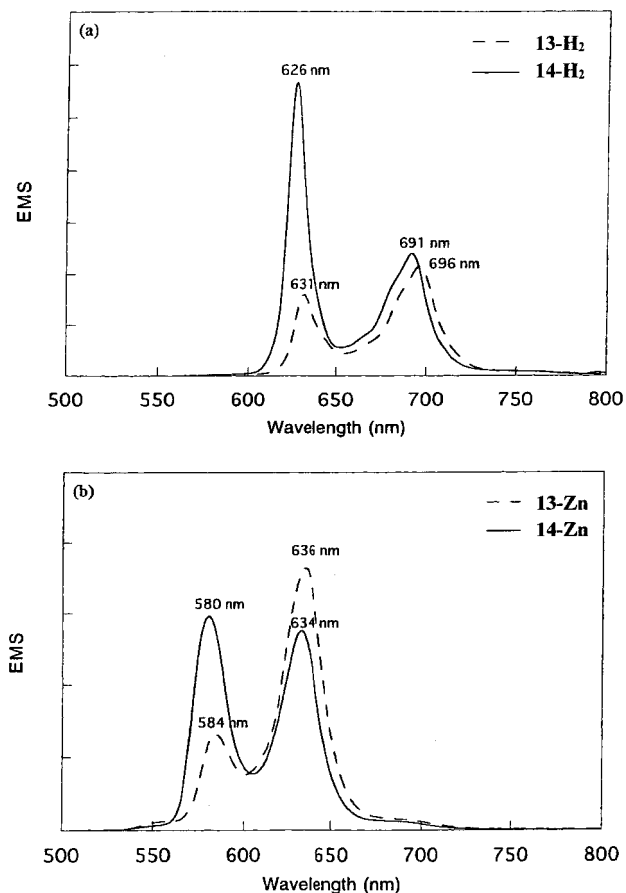


Figure 7. Emission spectra of (a) free base (**13**-H₂, **14**-H₂) and (b) Zn(II) (**13**, **14**) porphyrin in THF, which shows the peripheral substituent effects on the relative intensity ratio of vibronic emission bands.

~516 nm. In addition, the relatively larger dip in the transient absorption spectra around 650 nm is considered to arise from the stimulated emission of photoexcited free base porphyrin. The transient absorption spectra as well as the steady-state fluorescence data demonstrate that the energy transfer process from the photoexcited Zn(II) porphyrin to the free base porphyrin component occurs very fast and quantitatively (>99%). The representative kinetic profiles for transient absorption spectral changes for **1-P** at 516 nm, contributed by the free-base porphyrin transient, and 556 nm, contributed by the Zn(II) porphyrin transient, were shown in the inset of Figure 8a. In these plots, we only considered the pure bleaching amplitudes of Zn(II) and free base porphyrin transients by subtracting the broad and strong absorption tail of porphyrin ring (π, π^*) singlet excited states. The bleaching at ~556 nm contributed by photoexcited Zn(II) porphyrin unit decays with a lifetime of ~3.0 ps, and at its expense the bleaching at ~516 nm due mainly to free base porphyrin grows with the same time constant. The overall transient absorption spectral features and kinetic profiles of **1-P** and **1-M** ($(3.0 \text{ ps})^{-1}$, not shown) are quite similar to the analogous 1,4-phenylene hybrid diporphyrin investigated by Yang et al. ($(3.5 \text{ ps})^{-1}$).^{25b}

In the case of **1-O**,²³ the selective excitation of Zn(II) porphyrin unit can be attained although a relatively strong interaction between each constituent in this dimer causes more red-shift in Q-band and blue-shift in B-band. This spectral feature can be explained in terms of an enhanced excitonic coupling and π - π interaction between the two porphyrin rings in **1-O** dimer, but its interaction is weaker than **3-O**, which has an enforced slipped and face-to-face geometry with an average

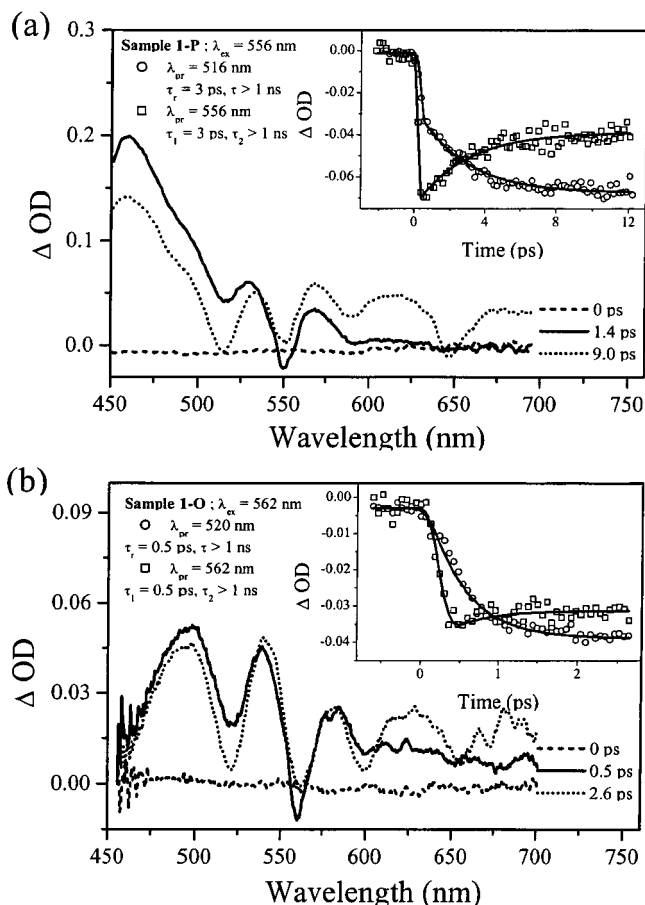


Figure 8. Transient absorption spectra of (a) **1-P** and (b) **1-O** at various time delays between pump and probe pulses after photoexcitation of Zn(II) porphyrin at 556 and 562 nm, respectively. Insets show their kinetic profiles for Zn(II) and free base pure bleaching, respectively.

distance of 3.4–3.5 Å.²⁶ In the case of **1-O**, the donor and acceptor moieties still maintain each electronic identity regardless of considerably mixed electronic character and the Zn(II) porphyrin unit can be preferentially photoexcited at 562 nm. The absorption band at 520 nm comes from the perturbed free base porphyrin unit. We observed the ground-state bleaching bands along with the envelope of a broad transient absorption in the time-resolved spectra, which show the same decay and rise time constant (~0.5 ps) in the kinetic profiles at 520 and 562 nm (Figure 8b and its inset). Development of the stimulated emission from photoexcited free base porphyrin at around 650 nm at 2.6 ps time delay clearly indicates the energy transfer from photoexcited Zn(II) porphyrin to free base porphyrin in this dimer with a time constant of 0.55 ps.

β -Octaalkyl-substituted Zn(II) porphyrin and free base diporphyrins (**3-P**, **3-M**, and **3-O**) connected by 1,4-, 1,3-, and 1,2-phenylene spacers were investigated to address the issue of interplay of frontier orbitals (a_{1u} vs a_{2u}) in the energy transfer process. β -Octaalkyl-substituted Zn(II) porphyrins are well-known to possess an A_{1u} HOMO orbital, in contrast with the A_{2u} HOMO orbital in TPP-type Zn(II) porphyrins (Scheme 3). This feature has been well characterized by the UV-visible absorption and ESR hyperfine splitting structures.³¹ In our previous studies, the rates of the intramolecular energy transfer in **3-P** and **3-M** have been determined to be $(15 \text{ ps})^{-1}$ and $(14 \text{ ps})^{-1}$, respectively, by picosecond single-photon counting technique,^{8f} but the time resolution of the used setup was insufficient to characterize these fast energy transfer processes. Therefore, this time we used femtosecond pump/probe transient

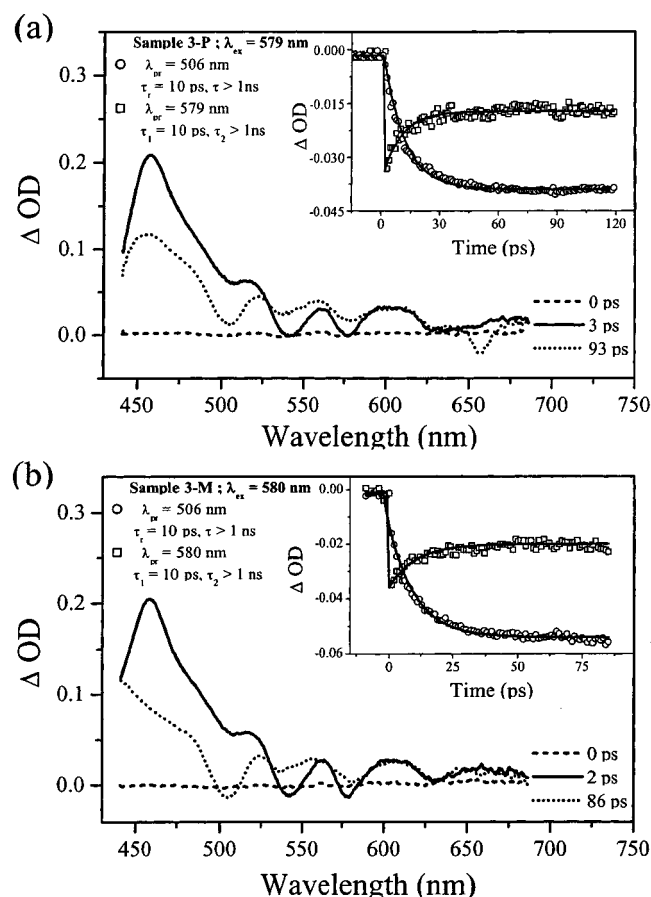


Figure 9. Transient absorption spectra of (a) **3-P** and (b) **3-M** at various time delays between pump and probe pulses after photoexcitation of Zn(II) porphyrin at 506 and 580 nm. Insets show their kinetic profiles for Zn(II) and free base pure bleaching, respectively.

absorption spectroscopy to obtain more accurate rate constants. The overall transient absorption spectrum at 3 ps delay time exhibits the bleaching of the Q(1,0) and weak Q(0,0) bands of Zn(II) porphyrin at ~ 543 and ~ 579 nm, respectively. This spectral feature suggests that the transient absorption spectrum at 3 ps time delay is primarily contributed by photoexcited Zn(II) porphyrin unit along with a small contribution from photoexcited free base porphyrin. This feature can be seen by a small bleaching signal at ~ 506 nm at 3 ps delay time, which is due to the $Q_y(1,0)$ ground-state absorption band of free base porphyrin. An increase in the delay time results in an increase in the contribution of free base porphyrin transients to the overall transient absorption spectrum as indicated by the growth of the 506 nm bleaching of free base porphyrin. At its expense, the bleaching signals at ~ 543 and ~ 579 nm by Zn(II) porphyrin diminishes with an increase in the time delay. At the longer time delay, the overall spectral feature is dominated by free base porphyrin, as characterized by the full growth of free base porphyrin bleaching bands at 506, 543, 579, and 628 nm and the stimulated emission from photoexcited free base porphyrin near 660 nm (Figure 9). The transient absorption spectra as well as the steady-state fluorescence data demonstrate that the energy transfer process from initially photoexcited Zn(II) porphyrin to free base porphyrin pigment occurs efficiently. The representative kinetic profiles for transient absorption spectral changes for **3-P** and **3-M** at 506 nm region, contributed by the free base porphyrin transients, and 579 nm, contributed by the Zn(II) porphyrin transients, were shown in the insets of Figure 9. As in the case of Figure 8, we only considered the bleaching

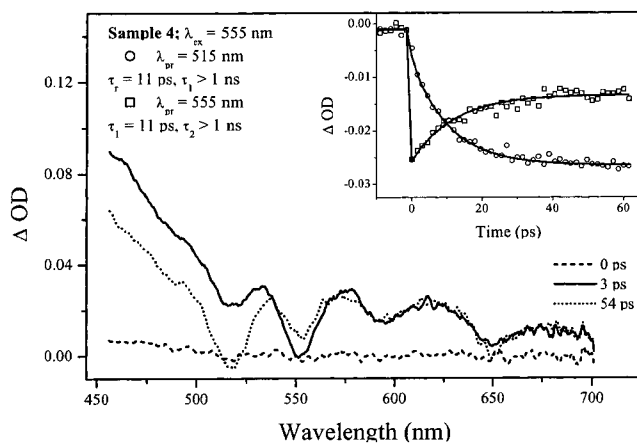


Figure 10. Transient absorption spectra of **4** at various time delays between pump and probe pulses after photoexcitation of Zn(II) porphyrin at 555 nm. Inset shows their kinetic profiles for free base and Zn(II) pure bleaching at 515 and 555 nm, respectively.

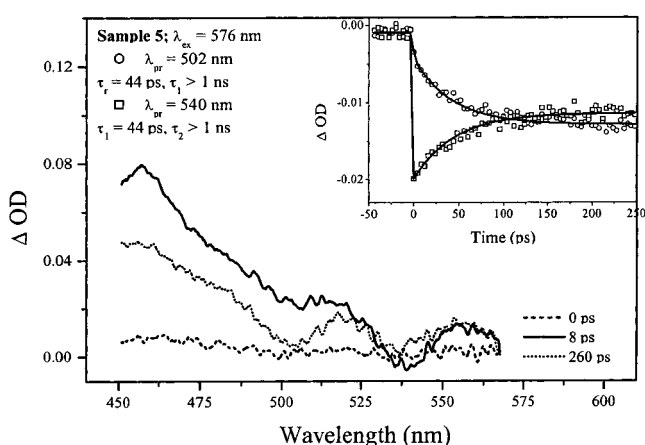


Figure 11. Transient absorption spectra of **5** at various time delays between pump and probe pulses after photoexcitation of Zn(II) porphyrin at 576 nm. Inset shows their kinetic profiles for free base and Zn(II) pure bleaching at 502 and 540 nm, respectively.

amplitudes of Zn(II) porphyrin and free base porphyrin transients by subtracting the broad and strong absorption tail of porphyrin ring (π, π^*) singlet excited states. The bleaching at ~ 579 nm contributed by photoexcited Zn(II) porphyrin unit decays with a lifetime of ~ 10 ps, and at its expense the bleaching at ~ 506 nm due mainly to free base porphyrin grows with the same time constant. Thus, our results indicate that the energy transfer rates in **3-P** and **3-M** are both $(\sim 10 \text{ ps})^{-1}$, which are approximately 3 times slower than those in **1-P** and **1-M** ($\sim 3.0 \text{ ps})^{-1}$.

Transient Absorption Spectra of 4,4'-Biphenylene-Bridged Diporphyrins. 4,4'-Biphenylene-linked Zn(II)-free base diporphyrins (**4** and **5**) show the Soret bands at 428 and 414 nm, respectively (Figures 3 and 4), which are less perturbed in comparison with those (431 and 420 nm) of **1-P** and **3-P** as shown in Figures 1 and 2. Smaller excitonic interactions in **4** and **5** are due to the larger distances between the porphyrin macrocycles. The steady-state fluorescence emission comes mainly from the free base porphyrin and, in a small portion, from the Zn(II) porphyrin, suggesting that the energy transfer is not quantitative.

In an analogous manner, the energy transfer reactions in **4** and **5** were studied by the transient absorption spectroscopy (Figures 10 and 11), reaching the results that the intramolecular energy transfer from the photoexcited Zn(II) to the free base porphyrin proceeds with a rate of $(11 \text{ ps})^{-1}$ and $(44 \text{ ps})^{-1}$ for **4**

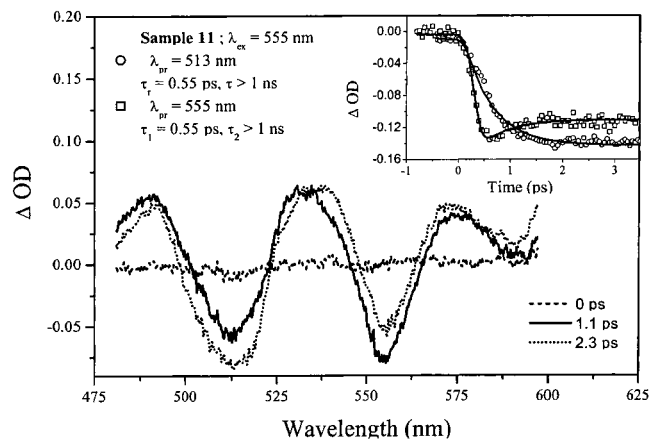


Figure 12. Transient absorption spectra of **11** in THF at various time delays between pump and probe pulses after photoexcitation of Zn(II) porphyrin at 555 nm. Inset shows their kinetic profiles for free base and Zn(II) pure bleaching at 513 and 555 nm, respectively.

and **5**, respectively. Thus, the energy transfer is ca. 4 times slower in **5** in comparison with **4**.

Transient Absorption Spectra of Meso–Meso Directly-Linked Diporphyrins. As ultimate spacerless models, similar experiments were carried out to characterize the energy transfer process in meso–meso directly-linked diporphyrin with a center-to-center distance of ~ 8.4 Å.³² At the early stage of the time delay, the transient absorption spectrum is mainly contributed by Zn(II) porphyrin transient after selective photopumping of Zn(II) porphyrin (Figure 12). The relative contribution of photoexcited free base porphyrin to the overall spectrum, however, is not negligible, as evidenced by the bleaching band in the 513 nm region. The spectral overlap between Zn(II) porphyrin and free base porphyrin at the pumping wavelength is similar to that in **1-P**. Thus, the larger contribution by free base porphyrin just after photoexcitation of the Zn(II) porphyrin unit in the transient absorption spectrum is likely to be due to very fast energy transfer. The representative kinetic profiles for transient absorption spectral changes for directly-linked Zn(II)-free base dimer at 513 nm, contributed by the free base porphyrin transients, and at 555 nm, contributed by the Zn(II) porphyrin transients, were shown in the inset of Figure 12. In these plots, the broad and featureless transient absorption arising from porphyrin ring singlet (π, π^*) state was corrected to consider only the bleaching amplitudes contributed by Zn(II) porphyrin and free base porphyrin transients, respectively. The bleaching at ~ 555 nm contributed by photoexcited Zn(II) porphyrin unit decays with a lifetime of ~ 0.55 ps, and at its expense the bleaching at ~ 513 nm due mainly to free base porphyrin grows with the same time constant, giving an energy transfer rate of $(0.55 \text{ ps})^{-1}$ in **11**.

The meso substituents of **11** are replaced with pentafluorophenyl groups in diporphyrin **12** with an expectation that the change of HOMO electronic nature from a_{2u} (TPP-type) to a_{1u} (OEP-type) has an influence on the energy transfer rate. The absorption spectrum shows the electronic interaction is diminished and the relative intensity ratio of emission vibronic bands changes in **12** (Figure 6). It is also shown in Figure 7 that the relative intensity of 0–0 vibronic band in **14-H₂** and **14-Zn** is observed to increase when the pentafluorophenyl groups are substituted, corresponding to the case that a_{2u} HOMO orbital (TPP-type) changes to a_{1u} HOMO orbital (OEP-type) (see Schemes 1–3). However, the energy transfer rate in **12** has been revealed to remain the same ($\sim 0.55 \text{ ps}^{-1}$) as that of **11** by the transient absorption spectra (Figure 13).

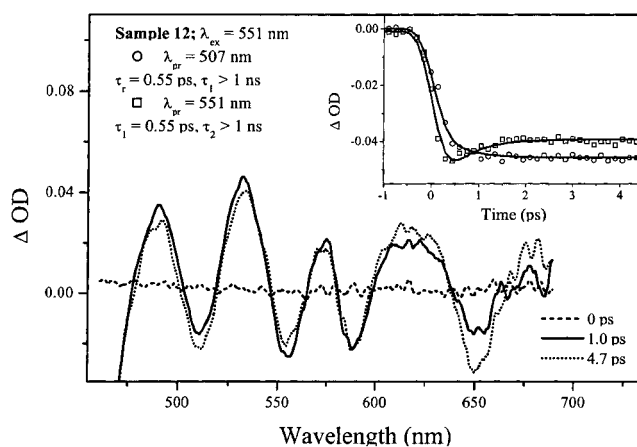


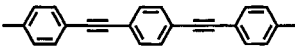
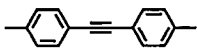
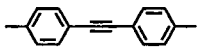
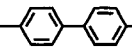
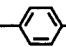
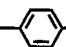
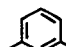
Figure 13. Transient absorption spectra of **12** in THF at various time delays between pump and probe pulses after photoexcitation of Zn(II) porphyrin at 551 nm. Inset shows their kinetic profiles for free base and Zn(II) pure bleaching at 507 and 551 nm, respectively.

IV. Discussion

Understanding of the key factors governing the energy transfer processes is crucial for the realization of truly efficient antenna molecular systems and signal transmitting molecular photonic devices. Development of efficient energy transfer components that equal the key energy transfer processes in the natural photosynthesis such as B800–B850 of LH2 is also an important issue in view of their incorporation into supramolecular multiporphyrin arrays. In principle, the electronic coupling can be provided by Coulombic interaction and electron exchange interaction, although the relative contributions differ case by case.^{11,12} The Coulombic interaction can be calculated in terms of the point-dipole approximation of dipole–dipole coupling for donor–acceptor pairs with large separations in the Förster mechanism¹¹ but can become increasingly larger in close proximity so as to drive ultrafast energy transfer such as those in B800–B850 in LH2¹⁶ and C-phycocyanine trimers¹⁴ or cause exciton-coupling induced spectral changes.¹³ Under such strongly interacting situations, the Coulombic interaction can be no more calculated by point-dipole approximation but should be treated by inclusion of multipole interactions.³³ As such, the mechanism of energy transfer depends on the magnitude of the electronic coupling and can be roughly classified into three cases: (1) the strong coupling case, (2) the intermediate coupling cases, and (3) the limit of the weak coupling case.³⁴ The strong coupling case corresponds to the excitonic coupling where the Franck–Condon state of the donor is instantaneously distributed over the orbital of the acceptor and thus the absorption spectra of the donor and acceptor are significantly influenced. The intermediate coupling cases may be further categorized into two: one is the partial exciton coupling in which the energy transfer occurs with partly retaining the oscillatory coherent feature but quickly loses its coherence due to vibrational and collisional perturbations, and the other one is the hot transfer mechanism in which the coherent feature is almost lost and the energy transfer occurs incoherently in competition with the vibrational relaxation. In the limit of the weak coupling case, the energy transfer occurs after completing the vibrational relaxation in the excited-state manifold, which is formulated as the Förster mechanism.¹¹

The energy transfer process principally mediated by the electron exchange interaction is formulated as the Dexter mechanism,¹² which should be effective only at a short distance for noncovalently-linked donor–acceptor pairs since it needs

TABLE 1: Intramolecular Energy Transfer Data

spacer	R (Å)	κ^2	compounds (A_{2u})		compounds (A_{1u})		ratio	
			k_{obs}^{-1} (ps)	$k_{\text{Förster}}^{-1}$ (ps)	k_{obs}^{-1} (ps)	$k_{\text{Förster}}^{-1}$ (ps)		
	26.6	1.125	156 (8)	3200	1750 (10)	1450	11	ref 19
	19.6	1.125	24 (6)	745	417 (9)	233	17	ref 17,18
	19.6	1.125	24 (6)	745	240 (7)	1326	10	ref 17,18
	17.0	1.1	11(4)	220	44 (5)	100	4	this work
	12.7	1.125	3 (1-P)	37	10 (3-P)	17	3	this work
	12.7	1.125	3 (1-P)	37	10 (2)	79	3	ref 25b
	11.0	0.531	3 (1-M)	33	10 (3-M)	15	3	this work
—	—	—	0.55 (11)	—	0.55 (12)	—	1	this work

the overlap of the wave function but can be often dominant for covalently-linked donor–acceptor pairs, since the covalent bonds between the donor and acceptor provide a way of transmission of the electron exchange interaction.³⁵ This through-bond mediated electronic coupling is dependent upon the frontier orbital characteristics of the spacer and should be large over π -conjugated spacers. As a result, the attenuation factors in the through-bond interactions over π -conjugated spacers are rather small, thereby realizing efficient energy transfer over long distances.^{17–19} Evaluating the relative contribution of the Coulombic interaction and the electron exchange interaction is a key to understand the mechanism of the energy transfer.

The Coulombic interaction can be approximated in terms of dipole–dipole interaction for donor–acceptor pairs with sufficiently large separations, resulting in the Förster eq 1,¹¹

$$k = \frac{8.8 \times 10^{-25} \kappa^2 \Phi}{n^4 R^6 \tau} \quad (1)$$

$$J = \int F(\nu) \epsilon(\nu) \nu^{-4} d\nu \quad (2)$$

in which n is the refractive index of the solvent, R is the center-to-center distance between donor and acceptor, Φ is the fluorescence quantum yield of the donor, κ is a dipole–dipole orientation factor, J is the spectral overlap integral, $F(\nu)$ is the normalized fluorescence spectrum of the energy donor, τ is the fluorescence lifetime of an energy donor, and $\epsilon(\nu)$ is the absorption spectrum of the energy acceptor with molar extinction coefficient ($\text{M}^{-1} \text{cm}^{-1}$) unit. The geometrical factors such as R and κ were estimated on the basis of optimized MM2 calculations. Calculations with eq 1 were performed for the diporphyrin models shown in Schemes 1 and 2 except the directly-linked diporphyrins **11** and **12** and 1,2-phenylene-bridged diporphyrins **1-O** and **3-O**, since their steady-state absorption and fluorescence spectra were significantly altered from those of the corresponding noncovalent reference porphyrin monomers, indicating that the energy transfer reactions in these models are lying outside the Förster mechanism. The calculated Förster rates

were listed in Table 1, in which the energy transfer rates of 1,4-bis(phenylethynyl)phenylene-linked diporphyrins **8** and **10**,¹⁹ and 1,4-diphenylethynylene-linked diporphyrins **6**,¹⁸ **7**,¹⁸ and **9**,¹⁷ are included for comparison.

In most cases, the intramolecular energy transfer is more efficient for TPP-type diporphyrins than the corresponding OEP-type diporphyrins. The observed differences are larger for diporphyrins bridged by long π -conjugated spacers such as 1,4-bis(phenylethynyl)phenylene (**8**^{19a} vs **9**^{19b}) and 1,4-diphenylethynylene (**6**¹⁸ vs **10**,¹⁷ and **6** vs **7**¹⁸). These spacers provide not only a well-defined large separation that leads to minimized through-space Coulombic interaction but also lower lying unoccupied molecular orbitals for mediating through-bond electronic coupling. Comparison of the energy transfer rates with the calculated Förster rates suggested that the through-bond interaction is dominant for the TPP-type diporphyrins **6** and **8**, is only of minor importance for the OEP-type diporphyrins **9** and **10**, and is modest for the model **7**. As shown in Scheme 3, the change of HOMO orbital from A_{2u} in **6** and **8** to A_{1u} in **7**, **9**, and **10** can explain these results.¹⁸ In addition, the phenyl group of the bridge is held nearly perpendicular to the porphyrin mean plane due to the flanking peripheral alkyl substituents in **9** and **10**, which decreases the electronic communication. The through-bond electronic interaction in **7** is inferred to be larger than that in **9**, since the energy transfer rate of **7** is larger than **9** despite its calculated smaller rate in the Förster mechanism. One possible reason may be the smaller dihedral angle between the porphyrin ring and the phenylene spacer in **7**. The ratio of the energy transfer rates in TPP-type diporphyrin vs OEP-type diporphyrin can be the measure of the relative contribution of the through-bond electronic interactions for the energy transfer.

Smaller spacers such as 4,4'-biphenylene, 1,4-phenylene, and 1,3-phenylene gave rise to larger energy transfer rates and smaller rate differences between TPP-type and OEP-type diporphyrins (**4** vs **5**), (**1-P** vs **3-P**), and (**1-M** vs **3-M**). With the decrease of the center-to-center separation, both the through-space Coulombic interaction and the through-bond exchange interaction should increase but the observed smaller rate

differences suggest the increasing relative contribution of the Coulombic interactions in the overall electronic interactions.

Comparison of the energy transfer rates of **11** and **12** would be interesting. We employed a 5,15-(pentafluoro)phenyl-substituted porphyrin as a reference with A_{1u} HOMO, since pentafluorophenyl group at the meso position is known to stabilize the a_{2u} orbital owing to its strong electron-withdrawing power.^{31b} Both the diporphyrins **11** and **12** exhibit the fluorescence spectra only coming from the free base porphyrins (Figure 6), indicating the quantitative energy transfer, but the fluorescence spectra are similar to those of the meso–meso-coupled free base diporphyrins, which are significantly altered from the corresponding monomer. This is arising from the exciton coupling in their close proximity with a center-to-center distance of 8.4 Å.²⁹ It is worth noting that the energy transfer rate in **11** is the same as that in **12**, since this result indicates that a change of electronic properties by the replacement of peripheral groups has no effect on the energy transfer rate despite the expected large through-bond electronic exchange interaction. One plausible explanation is that the Coulombic interaction is an overwhelmingly controlling factor over the through-bond interaction for the energy transfer in **11** and **12**. Here it is noteworthy again that despite the direct meso–meso linkage, the excited states of Zn(II) porphyrin and free base porphyrin can be treated as an individual separate state, thus allowing an extremely fast state-to-state energy transfer process. This feature, which is particularly desirable in its incorporation into supramolecular higher porphyrin arrays, most probably stems from its perpendicular conformation, which minimizes the electronic interactions between the porphyrins. Another merit of the directly-linked porphyrin arrays lies in their small conformational heterogeneity. The conformational heterogeneity of models causes the energy transfer rate to be nonexponential, which is expected to be more significant as the size of porphyrin arrays becomes larger. In this respect, the rigid structure of molecular arrays should be considered as a main concern in the fabrication of molecular photonic devices. Considering the small conformational heterogeneity and the very fast energy transfer, the meso–meso directly-linked diporphyrins such as **11** and **12** are useful and suitable synthetic molecular modules for the realization of molecular photonic devices based on the porphyrin arrays. In addition, the electronic effect of the linker cannot be disregarded in design strategy of molecular photonic devices, because the linker is also considered as a transmission element in electronic communication as described above.

Finally, the diporphyrins **1-O** and **3-O** with forced face-to-face geometries have the largest electronic interactions owing to the spatial proximity of the two porphyrin π -systems. The diporphyrin **1-O** shows a larger electronic coupling different from those of the diporphyrins **1-M** and **1-P**, exhibiting the blue-shifted B band (Figure 1c) and the observed fast energy transfer rate ($(0.5 \text{ ps})^{-1}$). But, it is also noted that the fluorescence spectrum of **1-O** is coming only from the free base porphyrin subunit and is only slightly perturbed, thus allowing the occurrence of a state-to-state energy transfer. In contrast, the diporphyrin **3-O** shows a very complicated absorption spectrum consisting of a blue-shifted, broad B band and featureless Q-bands as well as a red-shifted and rather broadened fluorescence, implying a considerable mixing of wave functions of the two porphyrins. Stronger electronic interactions in **3-O** than **1-O** is obvious. Since the through-bond electronic interaction must be smaller in **1-O** and **3-O** in comparison with those in **11** and **12**, the large electronic interaction in **1-O** and **3-O** is supplied via through-space interaction. The difference between

1-O and **3-O** can be ascribed to the peripheral substituents that play some roles in controlling the distance and π – π overlap area between the two porphyrin rings. A drastic change in the optical properties between **1-O** and **3-O** provides useful information on the boundary of the delocalized diporphyrin excimer state and two individually localized porphyrin excited states.

V. Conclusion

The intramolecular energy transfers in various Zn(II)-free base hybrid diporphyrin have been studied by the femtosecond time-resolved transient absorption spectroscopy with selective photopumping of Zn(II) porphyrin unit in the diporphyrins. The energy transfer rates increase tremendously as the center-to-center separation becomes shorter. Comparison of the energy transfer rates between A_{2u} -HOMO species (TPP-type) and A_{1u} -HOMO species (OEP-type and pentafluorophenyl-substituted TPP-type) is very informative on the relative contribution of the through-bond and the through-space interactions. The rate differences between the two species are large for the models bridged by linear π -conjugated spacers but become smaller with the decrease of the distance. The energy transfer rates are identical $(0.55 \text{ ps})^{-1}$ for the directly-linked meso–meso diporphyrins **11** and **12** regardless of the difference in the HOMO orbital symmetry characteristics, suggesting the predominant Coulombic interaction for the energy transfer in these close proximity porphyrin dimers over the through-bond electronic interactions via a meso–meso connecting single bond. 1,2-Phenylene spacers in **1-O** and **3-O** force compact face-to-face geometries of the two porphyrins but the choice of the peripheral substituents can lead to a state-to-state rapid energy transfer with a rate of $(0.55 \text{ ps})^{-1}$ for **1-O** or a delocalized excimer-like diporphyrin excited state for **3-O**.

Acknowledgment. The work at Yonsei University has been financially supported by the National Creative Research Initiatives Program of the Ministry of Science & Technology of Korea. Y.-R. Kim is thankful for the financial support from CRM-KOSEF grant (1998G0102), South Korea. The work at Kyoto was supported by Grant-in-Aids for Scientific Research (No.12874076, No. 12440196, and No. 11223205) from the Ministry of Education, Science, Sports, and Culture of Japan, and by CREST (Core Research for Evolutional Science and Technology) of Japan Science and Technology Corporation (JST).

Supporting Information Available: Detailed synthetic procedures and selected physical properties of all the models studied in this paper. This material is available free of charge via the Internet at <http://pubs.acs.org>.

References and Notes

- (1) (a) Wasielewski, M. R. *Chem. Rev.* **1992**, *94*, 435. (b) Gust, D.; Moore, T. A.; Moore, A. L. *Acc. Chem. Res.* **1993**, *26*, 198. (c) Speiser, S. *Chem. Rev.* **1996**, *96*, 1953. (d) Chou, J.; Kosal, M. E.; Nalwa, H. S.; Rakow, N. A.; Suslick, K. S. In *The Porphyrin Handbook*; Kadish, K. M.; Smith, K. M.; Guillard, R. Eds.; Academic Press: New York, 2000; Vol. 6, p. 43.
- (2) (a) Wagner, R. W.; Lindsey, J. S. *J. Am. Chem. Soc.* **1994**, *116*, 9759. (b) Prathapan, S.; Johnson, T. E.; Lindsey, J. S. *J. Am. Chem. Soc.* **1993**, *115*, 7519. (c) Wagner, R. W.; Lindsey, J. S.; Seth, J.; Palaniappan, V.; Bocian, D. F. *J. Am. Chem. Soc.* **1996**, *118*, 3996.
- (3) (a) Gosztola, D.; Yamada, H.; Wasielewski, M. R. *J. Am. Chem. Soc.* **1995**, *117*, 2041. (b) Debreczeny, M. P.; Svec, W. A.; Marsh, E. M.; Wasielewski, M. R. *J. Am. Chem. Soc.* **1996**, *118*, 8174. (c) Debreczeny, M. P.; Svec, W. A.; Wasielewski, M. R. *Science* **1996**, *274*, 584.
- (4) (a) Lin, V. S.-Y.; DiMagno, S. G.; Therien, M. J. *Science* **1994**, *264*, 1105. (b) Lin, V. S.-Y.; Therien, M. J. *Chem.-Eur. J.* **1995**, *1*, 645.

- (5) (a) Arnold, D. P.; Nitschinsk, L. *J. Tetrahedron* **1992**, *48*, 8781. (b) Arnold, D. P.; Heath, G. A.; James, D. A. *J. Por. Phthl.* **1999**, *3*, 5. (c) Anderson, H. L. *Inorg. Chem.* **1994**, *33*, 972. (d) Anderson, H. L. *Chem. Commun.* **1999**, 2323.
- (6) (a) Vicente, M. G. H.; Smith, K. M. *J. Org. Chem.* **1991**, *56*, 4407. (b) Vicente, M. G. H.; Jaquinod, L.; Smith, K. M. *Chem. Commun.* **1999**, 1771.
- (7) (a) Burrell, A. K.; Officer, D. L.; Reid, D. C. W. *Angew. Chem., Int. Ed. Engl.* **1995**, *34*, 900. (b) Burrell, A. K.; Officer, D. L. *Synlett.* **1998**, 1297.
- (8) (a) Osuka, A.; Liu, B.-L.; Maruyama, K. *Chem. Lett.* **1993**, 949. (b) Osuka, A.; Maruyama, K.; Mataga, N.; Asahi, T.; Yamazaki, I.; Tamai, N. *J. Am. Chem. Soc.* **1990**, *112*, 4958. (c) Osuka, A.; Nakajima, S.; Maruyama, K.; Mataga, N.; Asahi, T.; Yamazaki, I.; Nishimura, Y.; Ohno, T.; Nozaki, K. *J. Am. Chem. Soc.* **1993**, *115*, 4577. (d) Osuka, A.; Maruyama, K. *J. Am. Chem. Soc.* **1988**, *110*, 4454. (e) Osuka, A.; Maruyama, K.; Yamazaki, I.; Tamai, N. *J. Chem. Soc., Chem. Commun.* **1988**, 1243. (f) Osuka, A.; Maruyama, K.; Yamazaki, I.; Tamai, N. *Chem. Phys. Lett.* **1990**, *165*, 392.
- (9) (a) Ponomarev, G. V.; Borovkov, V.; Sugiura, K.; Sakata, Y.; Shul'ga, A. *Tetrahedron Lett.* **1993**, *34*, 2153. (b) Senge, M. O.; Gerzevske, K.; Vicente, M. G. H.; Forsyth, T.; Smith, K. M. *Angew. Chem., Int. Ed. Engl.* **1993**, *32*, 750. (c) Higuchi, H.; Takeuchi, M.; Ojima, J. *Chem. Lett.* **1996**, 593. (d) Sugiura, K.; Tanaka, H.; Matsumoto, T.; Kawai, T.; Sakata, Y. *Chem. Lett.* **1999**, 1193.
- (10) (a) Sessler, J. L.; Johnson, M. R. *Angew. Chem., Int. Ed. Engl.* **1987**, *26*, 678. (b) Sessler, J. L.; Capuano, V. L.; Harriman, A. *J. Am. Chem. Soc.* **1993**, *115*, 4618. (c) Brun, A. M.; Harriman, A.; Heitz, V.; Sauvage, J.-P. *J. Am. Chem. Soc.* **1991**, *113*, 8657. (d) Härberle, T.; Hirsch, J.; Pöllinger, F.; Heitele, H.; Michel-Beyerle, M. E.; Anders, C.; Döhl, A.; Krieger, C.; Rückemann, A.; Staab, H. A. *J. Phys. Chem.* **1996**, *100*, 18269. (e) Staab, H. A.; Carell, T. *Angew. Chem., Int. Ed. Engl.* **1994**, *33*, 1466.
- (11) (a) Förster, T. *Ann. Phys.* **1948**, *2*, 55 (b) Förster, T. *Discuss. Faraday Soc.* **1959**, *27*, 7.
- (12) Dexter, D. L. *J. Chem. Phys.* **1953**, *21*, 836.
- (13) van Grondelle, R.; Dekker, J. P.; Gillbro, T.; Sundström, V. *Biochim. Biophys. Acta* **1994**, *1187*, 1.
- (14) Gillbro, T.; Sharkov, A. V.; Kryukov, I. V.; Khoroshilov, E. V.; Kryukov, P. G.; Fischer, R.; Scheer, H. *Biochim. Biophys. Acta* **1993**, *1140*, 321.
- (15) (a) Breton, J.; Martin, J.-L.; Migus, A.; Antonetti, A.; Orszag, A. *Proc. Natl. Acad. Sci. U.S.A.* **1986**, *83*, 5121. (b) Jia, Y.; Jonas, D. M.; Joo, T.; Nagasawa, Y.; Lang, M. J.; Fleming, G. R. *J. Phys. Chem.* **1995**, *99*, 6263.
- (16) (a) McDermott, G. M.; Prince, S. M.; Freer, A. A.; Lawless, A. H. H.; Papiz, M. Z.; Cogdell, R. J.; Isaacs, N. W. *Nature* **1995**, *374*, 517. (b) Koepke, J.; Hu, X.; Muenke, C.; Schulten, K.; Michel, H. *Structure* **1996**, *4*, 581. (c) Pullerits, T.; Sundström, V. *Acc. Chem. Res.* **1996**, *29*, 381. (d) Sundström, V.; Pullerits, T.; van Grondelle, R. *J. Phys. Chem. B* **1999**, *103*, 2327. (e) van Oijen, A. M.; Ketelaars, M.; Köhler, J.; Aartsma, T. J.; Schmidt, J. *Science* **1999**, *285*, 400.
- (17) Osuka, A.; Tanabe, N.; Kawabata, S.; Yamazaki, I.; Nishimura, Y. *J. Org. Chem.* **1995**, *60*, 7177.
- (18) (a) Strachan, J. P.; Gentemann, S.; Seth, J.; Kalsbeck, W. A.; Lindsey, J. S.; Holten, D.; Bocian, D. F. *J. Am. Chem. Soc.* **1997**, *119*, 11191. (b) Yang, S. I.; Seth, J.; Balasubramanian, T.; Kim, D.; Lindsey, J. S.; Holten, D.; Bocian, D. F. *J. Am. Chem. Soc.* **1999**, *121*, 4008.
- (19) (a) Kawabata, S.; Yamazaki, I.; Nishimura, Y.; Osuka, A. *J. Chem. Soc., Perkin Trans 2* **1997**, 479. (b) Osuka, A.; Ikeda, M.; Shiratori, H.; Nishimura, Y.; Yamazaki, I. *J. Chem. Soc., Perkin Trans. 2* **1999**, 1019.
- (20) (a) Jensen, K. K.; van Berlekom, S. B.; Kajanus, K.; Martensson, J.; Albinsson, B. *J. Phys. Chem.* **1997**, *101*, 2218. (b) Kilsa, K.; Kajanus, J.; Martensson, J.; Albinsson, B. *J. Phys. Chem. B* **1999**, *103*, 7329. (c) Brodard, P.; Matzinger, S.; Vauthey, E.; Mongin, O.; Papamicael, C.; Gossauer, A. *J. Phys. Chem. A* **1999**, *103*, 5858.
- (21) (a) Hofmann, E.; Wrench, P. M.; Sharples, F. P.; Hiller, R. G.; Welte, W.; Diederichs, K. *Science* **1996**, *272*, 1788. (b) Krueger, B. P.; Scholes, G. D.; Jimenez, R.; Fleming, G. R. *J. Phys. Chem.* **1998**, *102*, 2284.
- (22) Debreczeny, M. P.; Wasielewski, M. R.; Shinoda, S.; Osuka, A. *J. Am. Chem. Soc.* **1997**, *119*, 6407.
- (23) 1,2-Phenylene-bridged TPP-type diporphyrin was first prepared by Kobuke et al., but its mono-zinc complex was not reported. Meier, H.; Kobuke, Y.; Kugimiya, S. *J. Chem. Soc., Chem. Commun.* **1989**, 923.
- (24) 1,3-Phenylene-bridged TPP-type diporphyrin was reported by Tabushi et al.: (a) Tabushi, I.; Sasaki, T. *Tetrahedron Lett.* **1982**, *23*, 1913. (b) Tabushi, I.; Sasaki, T. *J. Am. Chem. Soc.* **1983**, *105*, 2901. Preliminary results on intramolecular energy transfer were reported in ref 23 and the following paper: Meier, H.; Kobuke, Y.; Kugimiya, S. *Tetrahedron Lett.* **1989**, *30*, 5301.
- (25) 1,4-Phenylene-bridged TPP-type diporphyrin was first reported: (a) Wennerström, O.; Ericsson, H.; Raston, I.; Svensson, S.; Pimlott, W. *Tetrahedron Lett.* **1989**, *30*, 1129. Intramolecular energy transfer in 1,4-phenylene-bridged TPP-type Zn(II)-free base hybrid diporphyrin was reported: (b) Yang, S. I.; Lammi, R. K.; Seth, J.; Riggs, J. A.; Arai, T.; Kim, D.; Bocian, D. F.; Holten, D.; Lindsey, J. S. *J. Phys. Chem. B* **1998**, *102*, 9426.
- (26) 1,2-Phenylene-bridged OEP-type diporphyrin was prepared: Osuka, A.; Nakajima, S.; Nagata, T.; Maruyama, K.; Toriumi, K. *Angew. Chem., Int. Ed. Engl.* **1991**, *30*, 582.
- (27) 1,3-Phenylene-bridged OEP-type diporphyrin was reported: (a) Sessler, J. L.; Hugdahl, J.; Johnson, M. R. *J. Org. Chem.* **1986**, *51*, 2838. Osuka, A.; Maruyama, K. *J. Am. Chem. Soc.* **1988**, *110*, 4454. Intramolecular energy transfer in Zn(II)-free base hybrid diporphyrins was reported in: (b) Rodriguez, J.; Krimaier, C.; Johnson, M. R.; Friesner, R. A.; Holten, D.; Sessler, J. L. *J. Am. Chem. Soc.* **1991**, *113*, 1652, and ref 8f.
- (28) 1,4-Phenylene bridged OEP-type diporphyrin was reported in ref 9a and the intramolecular energy transfer in Zn(II)-free base hybrid diporphyrin was reported in refs 8f and 27b.
- (29) (a) Osuka, A.; Shimidzu, H.; *Angew. Chem., Int. Ed. Engl.* **1997**, *36*, 135. (b) Aratani, N.; Osuka, A.; Kim, Y. H.; Jeong, D. H.; Kim, D. *Angew. Chem., Int. Ed. Engl.* **2000**, *39*, 1458.
- (30) (a) Kasha, M. *Radiation Res.* **1963**, *20*, 55. (b) Kasha, M.; Rawls, H. R.; El-Bayoumi, M. A. *Pure Appl. Chem.* **1965**, *11*, 371.
- (31) (a) Gouterman, M. In *Porphyrins*; Dolphin, D., Ed.; Academic Press: New York, 1978; Vol. III, pp 1–165. (b) Spellane, J. P.; Gouterman, M.; Antipas, A.; Kim, S.; Liu, Y. C. *Inorg. Chem.* **1980**, *19*, 386. (c) Fujii, H. *Chem. Lett.* **1994**, 1491.
- (32) Cho, H. S.; Song, N. W.; Kim, Y. H.; Jeoung, S. C.; Hahn, S.; Kim, D.; Kim, S. K.; Yoshida, N.; Osuka, A. *J. Phys. Chem. A* **2000**, *104*, 3287.
- (33) Nagae, H.; Kakitani, T.; Mimuro, M. *J. Chem. Phys.* **1993**, *98*, 8012.
- (34) (a) Kakitani, T.; Kimura, A.; Sumi, H. *J. Phys. Chem. B* **1999**, *103*, 3720. (b) Kimura, A.; Kakitani, T.; Yamato, T. submitted to *J. Phys. Chem.*
- (35) (a) Zimmerman, H. E.; McKelvey, R. D. *J. Am. Chem. Soc.* **1971**, *93*, 3638. (b) Oevering, H.; Verhoeven, J. W.; Paddon-Row, M. N.; Cotsaris, E.; Hush, N. S. *Chem. Phys. Lett.* **1988**, *143*, 488. (c) Harriman, A.; Ziessel, R. *Chem. Commun.* **1996**, 1707.